Elastic light-emitting diode based on InGaN/GaN microwires and SWCNT/PDMS matrix electrode

© D.E. Kolesina[1], F.M. Kochetkov[1,2], A.A. Vorobyev[1], K.N. Novikova[1], A.S. Goltaev[1], I.S. Mukhin[1,2]

[1] St. Petersburg National Research Academic University of the Russian Academy of Sciences,
194021 St. Petersburg, Russia
[2] Peter the Great Saint-Petersburg Polytechnic University,
195251 St. Petersburg, Russia

E-mail: diana666167@gmail.com

Received March 26, 2025
Revised June 23, 2025
Accepted June 23, 2025

Presents the fabrication process of elastic light-emitting diode based on InGaN/GaN mircowires with „core-shell" structure encapsulated into commercial polydimethylsiloxane „Sylgard 184". In order to improve electrical and mechanical properties the matrix pixel electrodes — the addressing top and the general bottom — was established. Electro-optical perfomances was measured along to axis, and fabricated ligh-emitting diode demonstrates a blue light emission observed by human eyes and an able to stable work.

Keywords: Elastic electronics, blue LED, $A^{III}B^{V}$ microwires, PDMS, SWCNTs, optical lithography.

DOI: 10.61011/SC.2025.03.61556.7749

1. Introduction

Elastic optoelectronic devices are of interest to science and technology due to their wide application in wearable electronics [1,2], biomedical electronics [3–5] and in the clothing industry [6,7]. However, the organic light-emitting diode technology is the dominant technology in the market today. Organic materials are simple and inexpensive to produce, but they are not resistant to mechanical deformation, are susceptible to recrystallization and degradation of electrically conductive layers. In addition, organic light-emitting diodes emitting in the blue spectral range have low external quantum efficiency ($\sim 20\,\%$, [8]) and a rather short service life (5000 h compared to inorganic LEDs [9]), therefore, this technology is not suitable for devices where long-term operation at high brightness is required. The existing technology for the production of „micro-LED" displays, based on nitride semiconductor compounds, is superior in brightness and service life, but the technology requires careful post-processing, which affects the cost of the final device. At the same time, filamentous microcrystals of $A^{III}B^{V}$ exhibit high quantum efficiency, and a high aspect ratio of length to diameter provides excellent mechanical characteristics [10–12]. Filamentous microcrystals (FM) can be encapsulated in various silicone materials to give elasticity to a light-emitting device. Since such devices are capable of stretching, they require stretchable electrodes. Single-walled carbon nanotubes (SWCNT) obtained by aerosol chemical vapor deposition [13–15] with a transparency of 80% (at a wavelength of 550 nm) have proven themselves as stretchable electrodes. It was shown in Ref. [16] that SWCNT deposited on polydimethylsiloxane films (PDMS), retain their performance characteristics under tension and have a stable electrical contact to the filamentous microcrystal. In addition, a pattern is applied using optical lithography to preserve electrical conductivity and optical transparency during stretching [16].

This study is devoted to the creation and research of a blue stretchable LED based on a stretchable SWCNT electrode/PDMS produced by projection optical lithography, the electrophysical, optical and radiometric characteristics of the resulting LED were measured. The LED demonstrates stable operation when stretched by 10 % along two axes.

2. Experimental part

2.1. The growth of self-organized InGaN/GaN filamentous microcrystals

The self-organized InGaN/GaN filamentous microcrystal structures „core-shell" were grown by deposition of organometallic reagents from the gas phase on a sapphire substrate [17]. Growth consists of several stages. At the first stage, filamentous GaN nanocrystals with a height of $\sim 10\,\mu$m were grown at a low ratio of flows of N to Ga and In (~ 50) and at high flow rate of silane ~ 200 nmol/min, temperature of $\sim 1050\,^{\circ}$C and at a pressure of 800 mbar. A passivating layer SiN_x formed around the core leg. Further, growth was continued without a silane flow, and unalloyed GaN was grown (height $\sim 15\,\mu$m, growth time ~ 300 s). Seven InGaN quantum wells (the scheme of the grown filamentous microcrystal is shown in Figure 1, *a*) were grown by lowering the growth temperature from 1050 to 750 °C. The growth was suppressed in the lower part of the filamentous microcrystal due to the presence of a passivating layer. The quantum wells were separated by GaN layers, and further growth was carried out at a temperature of 885 °C at a

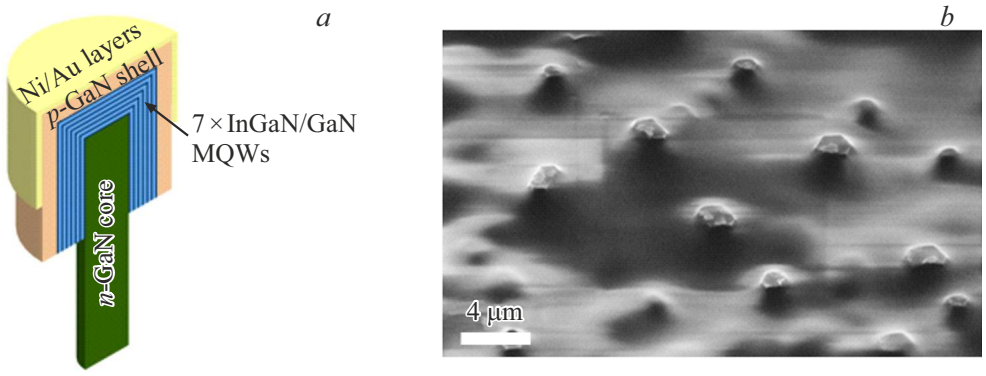

Figure 1. *a* — scheme of single filamentous microcrystal with InGaN/GaN quantum wells; *b* — an encapsulated array of filamentous microcrystals in the PDMS.

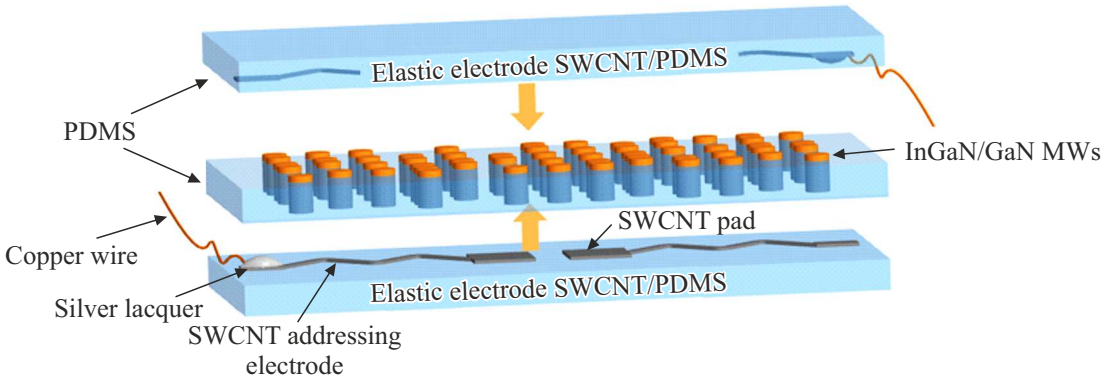

Figure 2. Schematic diagram of an elastic LED based on InGaN/GaN filamentous microcrystals and an SWCNT/PDMS elastic electrode.

pressure of 400 mbar. The growth was completed by the formation of *p*-GaN shell with a thickness of ~ 70 nm at a temperature of 720 °C, followed by annealing for 20 min of the alloying impurity.

2.2. Manufacturing of the filamentous microcrystal/PDMS light-emitting membrane

To establish ohmic contact between the deposited layers of SWCNT and the *p*-GaN shell, layers of Ni/Au metal with a thickness of 5 nm were deposited on the upper parts of InGaN/GaN filamentous microcrystals by vacuum thermal evaporation. After metallization, the InGaN/GaN array was annealed in an atmosphere at a temperature of 500 °C for 15 min. The array was then encapsulated in a commercial silicone polymer PDMS „Sylgard 184“ by gravity winding (Figure 1, *b*) [18–20]. After encapsulation, the sample was kept in a drying cabinet at 80 °C for 1 h. The sample was etched in plasma O_2 to remove the wetting layer from the upper parts of the filamentous microcrystal. The flow O_2 was 250 ml/s, the etching time was 60 seconds, and the gas discharge power was 500 watts. The blue InGaN/GaN filamentous microcrystal/PDMS LED membrane was then mechanically separated from the rigid sapphire substrate by a microtomic blade.

2.3. Manufacture of an SWCNT/PDMS elastic electrode

SWCNT/PDMS elastic electrode was produced using projection lithography using a sacrificial layer [16]. The electrode consists of an address electrode in the form of a meander and 8 squares with dimensions of $1 \times 1\,mm^2$ (Figure 2). The SWCNT used in the study were synthesized by aerosol chemical deposition from the gas phase [14]. The SWCNT film was deposited on a nitrocellulose filter at the outlet of the reactor. The transparency of the SWCNT used in this study is 80% at a wavelength of 550 nm and it has a layer resistance of 20 Ohm/sq. [15].

SWCNT/PDMS elastic electrodes were mechanically transferred to the upper and lower sides of the InGaN/GaN filamentous microcrystal/light-emitting membrane PDMS. For the convenience of assembling and aligning the electrodes on the membrane surface, the electrodes were placed on a glass substrate, the alignment accuracy is $\pm 100\,\mu m$. The substrate was removed after assembly. For the convenience of measurements, drops of silver varnish were applied to the output pads of the electrodes, in which the copper wiring was placed. The manufacturing scheme of the device is shown in Figure 2.

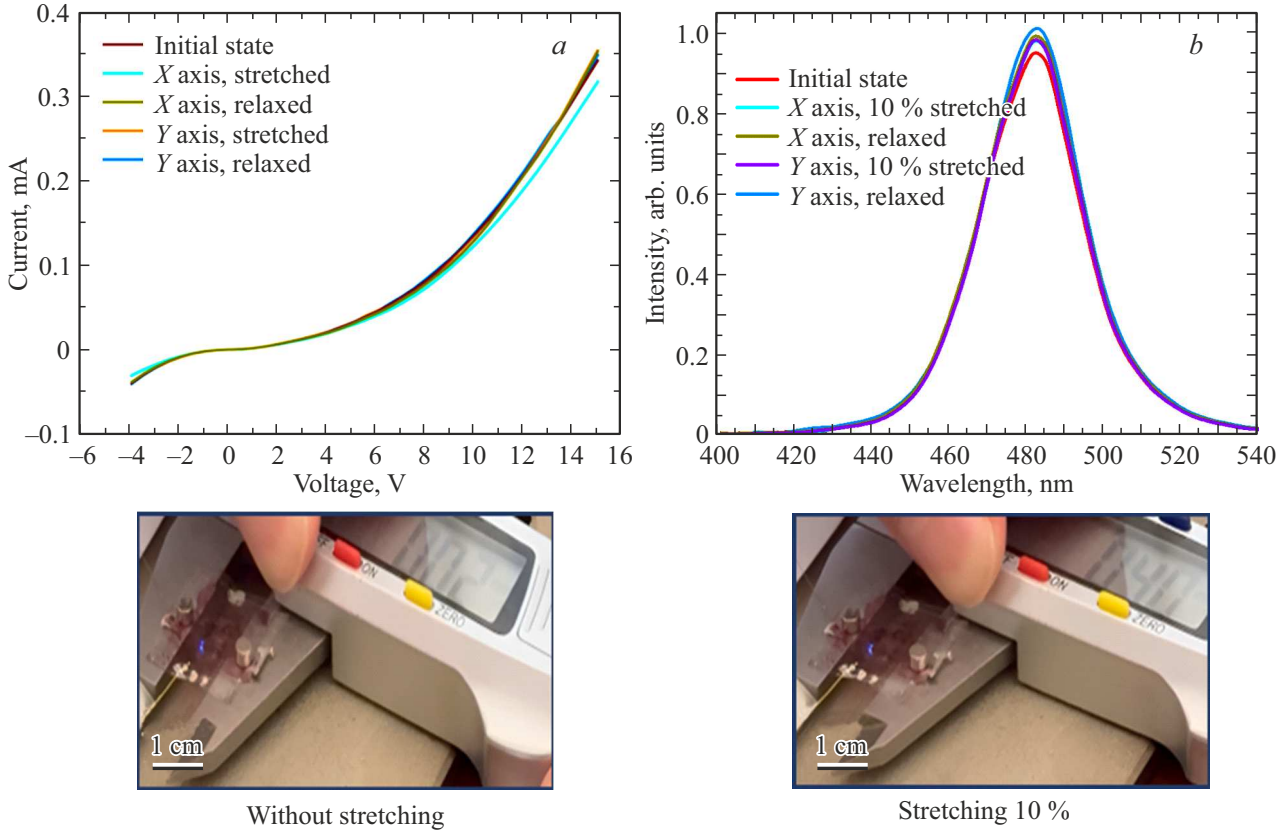

Figure 3. *a* — current-voltage curve of an elastic LED when stretched along the axes *X* and *Y* at 10 % and after it; *b* — electroluminescence spectra of an elastic LED when stretched along the axes *X* and *Y* at 10 % and after it. The inserts show how the device works when stretched.

3. Results and discussion

3.1. Measurement of electrophysical and optical characteristics of an LED

The current-voltage curve of the LED were measured before and after stretching along two axes to prove the electrical stability of elastic electrodes with a light-emitting membrane (Figure 3, *a*). To do this, an elastic LED was mounted on a caliper using neodymium magnets (the accuracy of the caliper is ~ 0.05 mm). The measured current-voltage curve are shown in Figure 3, *a*. The opening voltage of the LED is 5 V. The LED current is ~ 0.35 mA at 15 V. The current decreased slightly to ~ 0.33 mA ($< 5\%$) during the first stretching along the *X* axis. However, it is worth noting that the subsequent relaxation along the *Y* axis did not lead to a further deterioration in electrical characteristics. The current density at an applied voltage of 15 V was ~ 3 A/cm^2 for the studied LED. The opening voltage did not change during stretching, which indicates stable contact between the elastic electrodes and the InGaN/GaN filamentous microcrystal-based membrane. The current drop during the first stretching may be due to the mechanical stabilization of the electrical contact between the SWCNT and InGaN/GaN filamentous microcrystal during the initial stretching. In addition, drops of silver varnish could lead to local mechanical instability of the contacts during stretching.

Then the electroluminescence spectra were measured when stretched along two axes by 10 % and after it. The electroluminescence spectra were measured at a voltage of 15 V (Figure 3, *b*). Stable electroluminescence can be observed from the spectra at a wavelength of 482 nm, which corresponds to the blue spectral range. It is worth noting that the primary stretching/relaxation cycles along the axes *X* and *Y* did not cause significant changes in the intensity of electroluminescence. A slight increase in the intensity of electroluminescence can be explained by an improvement in the electrical contact between the SWCNT and the InGaN/GaN filamentous microcrystal membrane. Also, stretching had no effect on the position of the peaks and the shape of the spectrum, which indicates the stable operation of the elastic LED.

In addition, the radiometric characteristics of the device were measured (Figure 4) before stretching by 10% along one of the axes and after. Radiometric measurements also confirm the presence of stable contact between the SWCNT and the InGaN/GaN filamentous microcrystal membrane, since it does not change significantly over time. The increase in power during the initial stretching of the device also

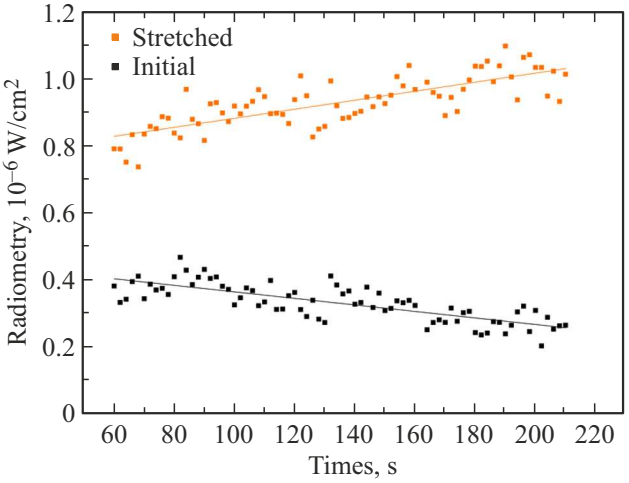

Figure 4. Radiometric characteristics of the InGaN/GaN filamentous microcrystal/SWCNT/PDMS elastic LED.

indicates an improvement in the electrical contact between the SWCNT and the InGaN/GaN filamentous microcrystal.

4. Conclusion

An elastic LED was produced in the course of the study based on stretchable electrodes PDMS/SWCNT obtained by projection optical lithography and a light-emitting membrane based on InGaN/GaN filamentous microcrystals and PDMS. During the measurements, the electrical stability of the LED was demonstrated when stretched by 10 % along two axes and when further relaxed. This stability indicates the resistance of the electrodes to cyclic loads, which is of great importance when creating various flexible electronics.

Funding

The study was supported by the Ministry of Education and Science of the Russian Federation, grant No. FSRM-2023–0007.

Conflict of interest

The authors declare that they have no conflict of interest.

References

[1] J. Heikenfeld, A. Jajack, J. Rogers, P. Gutruf, L. Tian, T. Pan, R. Li, M. Khine, J. Kim, J. Wang, J. Kim. Lab Chip, **18**, 217 (2018).
[2] M. Kong, M. Yang, R. Li, Y.-Z. Long, J. Zhang, X. Huang, X. Cui, Y. Zhang, Z. Said, C. Li. Int. J. Adv. Manufact. Technol., **131**, 3205 (2024).
[3] Z. Zhou, K. Chen, X. Li, S. Zhang, Y. Wu, Y. Zhou, K. Meng, C. Sun, Q. He, W. Fan, E. Fan, Z. Lin, X. Tan, W. Deng, J. Yang, J. Chen. Nature Electronics, **3**, 571 (2020).
[4] A. Yu, M. Zhu, C. Chen, Y. Li, H. Cui, S. Liu, Q. Zhao. Adv. Healthcare Mater., **13** (2), 2302460 (2024).
[5] Y. Du, J.H. Kim, H. Kong, A.A. Li, M.L. Jin, D.H. Kim, Y. Wang. Adv. Healthcare Mater., **13** (16), 2303461 (2024).
[6] S.A. Behera, S. Panda, S. Hajra, K.R. Kaja, A.K. Pandey, A. Barranco, S.M. Jeong, V. Vivekananthan, H.J. Kim, P.G.R. Achary. Adv. Sustainable Systems, **8** (12), 2400344 (2024).
[7] T. Blecha, M. Hirman, J. Navratil. Power Electronic Dev. Components, **7**, 100056 (2024).
[8] A. Salehi, X. Fu, D. Shin, F. So. Adv. Funct. Mater., **29** (15), 1808803 (2019).
[9] A. Sugimoto, H. Ochi, S. Fujimura, A. Yoshida, T. Miyadera, M. Tsuchida. IEEE J. Select. Top. Quant. Electron., **10**, 107 (2004).
[10] X. Dai, A. Messanvi, H. Zhang, C. Durand, J. Eymery, C. Bougerol, F.H. Julien, M. Tchernycheva. Nano Lett., **15**, 6958 (2015).
[11] N. Guan, X. Dai, A. Messanvi, H. Zhang, J. Yan, E. Gautier, C. Bougerol, F.H. Julien, C. Durand, J. Eymery, M. Tchernycheva. ACS Photonics, **3**, 597 (2016).
[12] L. Güniat, P. Caroff, A. Fontcuberta i Morral. Chem. Rev., **119**, 8958 (2019).
[13] Q. Zhang, N. Wei, P. Laiho, E.I. Kauppinen. Top. Curr. Chem. Collections, **375**, 90 (2017).
[14] A.G. Nasibulin, P.V. Pikhitsa, H. Jiang, D.P. Brown, A.V. Krasheninnikov, A.S. Anisimov, P. Queipo, A. Moisala, D. Gonzalez, G. Lientschnig, A. Hassanien, S.D. Shandakov, G. Lolli, D.E. Resasco, M. Choi, D. Tománek, E.I. Kauppinen. Nature Nanotechnol., **2**, 156 (2007).
[15] E.P. Gilshteyn, S.A. Romanov, D.S. Kopylova, G.V. Savostyanov, A.S. Anisimov, O.E. Glukhova, A.G. Nasibulin. ACS Appl. Mater. Interfaces, **11**, 27327 (2019).
[16] S. Mukhangali, V. Neplokh, F. Kochetkov, A. Vorobyev, D. Mitin, M. Mukhin, D.K. Krasnikov, J. Tian, R. Islamova, A.G. Nasibulin, I. Mukhin. Appl. Phys. Lett., **121** (24), 243504 (2022).
[17] R. Koester, J.S. Hwang, C. Durand, D. Le Dang, J. Eymery. Nanotechnology, **21** (1), 015602 (2010).
[18] F.M. Kochetkov, V. Neplokh, V.V. Fedorov, A.D. Bolshakov, V.A. Sharov, I.E. Eliseev, M. Tchernycheva, G.E. Cirlin, A.G. Nasibulin, R.M. Islamova, I.S. Mukhin. Nanotechnology, **31**, 46LT01 (2020).
[19] V. Neplokh, F.M. Kochetkov, K.V. Deriabin, V.V. Fedorov, A.D. Bolshakov, I.E. Eliseev, V.Yu. Mikhailovskii, D.A. Ilatovskii, D.V. Krasnikov, M. Tchernycheva, G.E. Cirlin, A.G. Nasibulin, I.S. Mukhin, R.M. Islamova. J. Mater. Chem. C, **8**, 3764 (2020).
[20] F.M. Kochetkov, V. Neplokh, V.A. Mastalieva, S. Mukhangali, A.A. Vorob'ev, A.V. Uvarov, F.E. Komissarenko, D.M. Mitin, A. Kapoor, J. Eymery, N. Amador-Mendez, C. Durand, D. Krasnikov, A.G. Nasibulin, M. Tchernycheva I.S. Mukhin. Nanomater., **11**, 1503 (2021).

Translated by A.Akhtyamov